



UNIVERSITY OF LEEDS

This is a repository copy of *Silence on Shangri-La: attenuation of Huygens acoustic signals suggests surface volatiles*.

White Rose Research Online URL for this paper:
<http://eprints.whiterose.ac.uk/80312/>

Version: Accepted Version

Article:

Lorenz, RD, Leese, MR, Hathi, B et al. (6 more authors) (2014) Silence on Shangri-La: attenuation of Huygens acoustic signals suggests surface volatiles. *Planetary and Space Science*, 90. 72 - 80. ISSN 0032-0633

<https://doi.org/10.1016/j.pss.2013.11.003>

Reuse

Unless indicated otherwise, fulltext items are protected by copyright with all rights reserved. The copyright exception in section 29 of the Copyright, Designs and Patents Act 1988 allows the making of a single copy solely for the purpose of non-commercial research or private study within the limits of fair dealing. The publisher or other rights-holder may allow further reproduction and re-use of this version - refer to the White Rose Research Online record for this item. Where records identify the publisher as the copyright holder, users can verify any specific terms of use on the publisher's website.

Takedown

If you consider content in White Rose Research Online to be in breach of UK law, please notify us by emailing eprints@whiterose.ac.uk including the URL of the record and the reason for the withdrawal request.



eprints@whiterose.ac.uk
<https://eprints.whiterose.ac.uk/>

1
2
3
4
5
6
7
8
9
10 Silence on Shangri-La : Detection of Titan Surface Volatiles by Acoustic
11
12
13 Absorption in Huygens Probe Measurements
14
15
16
17
18
19
20
21
22
23

24
25 Ralph D. Lorenz*, Johns Hopkins University Applied Physics Laboratory, Laurel, MD 20723, USA
26

27
28 Mark R. Leese, Brijen Hathi, John C. Zarnecki, Axel Hagermann, The Open University, Milton
29
30 Keynes, UK
31
32

33
34 Phil Rosenberg, University of Leeds, Leeds, UK
35
36

37
38 Martin C. Towner, Department of Applied Geology, Curtin University, Perth, Australia
39

40
41 James Garry, Red Core Consulting, Burnaby, British Columbia, Canada
42
43

44
45 Håkan Svedhem, European Space Agency, ESTEC, Noordwijk, The Netherlands
46
47
48
49
50

51
52 ~~Submitted to Planetary and Space Science, July 23, 2013~~
53

54
55 * corresponding author. Tel. +1 443 778 2903 Fax. +1 443 778 8939 ralph.lorenz@jhuapl.edu
56

57
58 Lorenz, R. D., M. R. Leese, J. C. Zarnecki, A. Hagermann, P. Rosenberg, M.
59 Towner, J. Garry and H. Svedhem, Silence on Shangri-La : Detection of Titan
60 Surface Volatiles by Acoustic Absorption, Planetary and Space Science, 90,
61 72–80, 2014
62
63
64
65

1
2
3
4
5
6
7
8
9 Objective:

10
11
12 Characterize and understand acoustic instrument performance on the surface of Titan
13
14

15
16 Methods:

17
18
19 The Huygens probe measured the speed of sound in Titan's atmosphere with a 1MHz pulse
20
21
22 time-of-flight transducer pair near the bottom of the vehicle. We examine the fraction of
23
24
25 pulses correctly received as a function of time.
26
27

28 Results :

29
30
31 This system returned good data from about 11km altitude, where the air became thick enough
32
33
34 to effectively transmit the sound, down to the surface just before landing : these data have
35
36
37 been analyzed previously. After an initial transient at landing, the instrument operated
38
39
40 nominally for about 10 minutes, recording pulses much as during descent. The fraction of
41
42
43 pulses detected then declined and the transmitted sound ceased to be detected altogether,
44
45
46 despite no indication of instrument or probe configuration changes.
47
48
49
50

51 Conclusions:

52
53
54 The most likely explanation appears to be absorption of the signal by polyatomic gases with
55
56
57 relaxation losses at the instrument frequency, such as ethane, acetylene and carbon dioxide.
58

59
60 These vapors, detected independently by the GCMS instrument, were evolved from the surface
61
62
63
64
65

1
2
3
4
5 material by the warmth leaking from the probe, and confirm the nature of the surface materials
6
7
8 as 'damp' with a cocktail of volatile compounds. Some suggestions for future missions are
9
10 considered.
11
12
13
14
15
16

17 Practice Implications :

18
19
20
21 None.
22
23

24 Keywords : Instrumentation ; Acoustics ; Planetary Atmospheres ; Organic Chemistry ;

25
26
27 Attenuation ; Huygens Probe
28
29
30
31
32
33
34
35
36
37
38
39
40
41
42
43
44
45
46
47
48
49
50
51
52
53
54
55
56
57
58
59
60
61
62
63
64
65

1. Introduction

Titan is unique among the satellites of the solar system in that it has an atmosphere. This makes it of particular interest to acousticians (e.g. Leighton and White, 2005; Leighton and Petculescu, 2009) since the propagation of sound is of interest in its own right, both for education/outreach as well as for science, as well as serving as a means to study winds and transient phenomena such as precipitation, wave breaking, thunder, volcanic eruptions and bolide entry. Titan's thick atmosphere is favorable for the generation and receipt of soundwaves by transducers, and the low temperatures make the attenuation by the constituent gases relatively low(e.g. Petcelescu and Lueptow, 2007; Hanford et al., 2009).

Although the Cassini spacecraft in Saturn orbit continues to make remarkable findings at Titan and motivates future in-situ exploration by landers, balloons or other platforms, the only available in-situ environmental data from Titan's surface is that from the Huygens probe, from which data were received for 72 minutes after its landing at the western margins of the Shangri-La dunefields near Titan's equator. It is therefore important to examine these data, hard-won from Titan's cryogenic environment, for whatever insights they may offer - even when the data were not necessarily acquired through the expected operation of the relevant instrumentation. Since a number of proposed future investigations have considered ultrasonic anemometers, depth sounders, and passive microphones, we therefore examine the surface operation of the Huygens acoustic instrumentation, whose results were not interpreted previously.

1
2
3
4
5
6 The Huygens probe to Titan carried three acoustic instruments. A passive microphone, part of
7
8 the Huygens Atmospheric Structure Instrument (HASI) was intended to search for thunder, but
9
10 detected only aeroacoustic noise during descent. The Surface Science Package (SSP) carried a
11
12 down-pointing sonar, the Acoustic Properties Instrument - Sounder (API-S) which detected an
13
14 echo from the surface during the last seconds of parachute descent (Zarnecki et al., 2005;
15
16 Towner et al., 2007), and a speed-of-sound sensor (Acoustic Properties Instrument - Velocity, or
17
18 API-V). It is this latter instrument that forms the topic of the present paper.
19
20
21
22
23
24
25
26
27

28 2. Instrumentation

29
30
31 When the Huygens probe was conceived, a prevailing model for Titan's surface was of a global
32
33 ocean and, while post-landing survival was not guaranteed, the possibility of making brief
34
35 measurements on the surface was recognized. The probe specification demanded that it float,
36
37 and that the battery energy and communications budgets permit at least 3 minutes of surface
38
39 operations. One quick measurement that was included as a diagnostic of the methane:ethane
40
41 ratio in the ocean was a speed of sound measurement, implemented within the Surface Science
42
43 Package (SSP) on the probe (Zarnecki et al., 1997). This measurement (as others such as
44
45 dielectric constant and refractive index in the SSP) required sensors to be immersed in the
46
47 ocean, and so these were mounted near the apex of the probe (figure 1).
48
49
50
51
52
53
54
55
56
57
58

59 < Figure 1 >
60
61
62
63
64
65

1
2
3
4
5
6
7
8
9 The speed of sound measurement on Huygens was very simple in concept : a pair of
10 transducers are separated by a known distance (12.7cm), and the propagation time of a pulse
11 of ultrasound (1MHz) across that distance is measured by starting a clock on emission at one
12 transducer and stopping it on receipt at the other. In practice (e.g. Rosenberg 2008;
13 Hagermann et al., 2007) the simple design using a threshold detector on the receive circuit led
14 to some subtleties in performance.
15
16
17
18
19
20
21
22
23
24

25 The principal objective of the measurement was to diagnose liquid composition, and to provide
26 a sound speed to permit the echo delay time from a small acoustic depth-sounder to be
27 interpreted as an ocean depth. During development it was realized that meaningful data might
28 also be obtained during descent (e.g. Lorenz, 1994; Garry, 1996; Zarnecki et al., 1997; Svedhem
29 et al., 2004).
30
31
32
33
34
35
36
37
38
39
40
41

42 The instrument consisted of two sensor heads (API-V1 and API-V2) each containing a
43 piezoelectric element (PXE-5) able to act as both a transmitter and a receiver. The sensor heads
44 were mounted opposite and facing each other across the SSP cavity (figure 2) allowing
45 atmospheric gases to flow past them. The sensors were mounted at the opening of the cavity,
46 but behind an electromagnetic shield (figure 3) designed to prevent damage to the
47 instrumentation from any lightning or electrostatic discharge.
48
49
50
51
52
53
54
55
56
57
58
59
60
61
62
63
64
65

1
2
3
4
5 To make a measurement, a 1-MHz wavetrain of nominally 10 μs duration (i.e. 10 cycles) was
6 transmitted between the sensors and the time of flight of this sound wave was measured. The
7 timing clock had a frequency of 4 MHz giving a time resolution for the measurement of 0.25 μs .
8
9 This process was repeated twice per second (once in each direction) potentially providing
10 metre-scale vertical resolution during the descent through Titan's atmosphere.
11
12
13
14
15
16
17
18
19
20

21 Experimentation with flight spare sensors revealed that it takes a time $t_0 = 3.71 \mu\text{s}$ for the
22 sound waves to propagate out of the transmitting sensor and into the receiving sensor,
23 assuming zero free-space separation. It is clear that this value of t_0 is determined by the
24 capacitance of the piezoelectric crystals as well as the thickness of, and speed of sound within,
25 the crystals and their impedance matching coatings.
26
27
28
29
30
31
32
33
34
35

36 Experimentation with flight spare sensors also revealed that the envelope of the received signal
37 is more bell shaped than the transmitted signal. This effect, due to the resonant response of the
38 transducer with finite Q , means that early peaks in the signal train may not have large enough
39 amplitude to be detected. Each peak missed in this way causes API-V to overestimate the time
40 of flight by 1 μs . Before encounter it was expected that, as the probe descended and the
41 density of the atmosphere increased, the received signal would become stronger and fewer
42 peaks would be missed in this way. This would manifest itself in the flight data in the form of
43 discontinuities separated by 1 μs in a plot of time of flight vs altitude.
44
45
46
47
48
49
50
51
52
53
54
55
56
57
58
59
60
61
62
63
64
65

1
2
3
4
5
6 Given the trigger voltage threshold on the flight sensor of 69.9 mV, operation was expected to
7
8 require a transmission coefficient of at least $\sim 0.315 \times 10^{-3}$ which, using room temperature data
9
10 for the sensor materials, corresponds to a required impedance of the sampled gas of at least
11
12 ~ 629 Rayl. Examining the predicted engineering model for Titan's atmosphere, it should have
13
14 been expected that the sensor would begin to operate at around 10-12 km altitude.
15
16
17
18
19
20
21
22

23
24 < Figure 2 >
25
26
27
28
29

30
31 < Figure 3
32
33

34 3. Data

35
36
37 The data analyzed here are the propagation times measured by the API-V instrument during the
38
39 descent, as calibrated and archived on the NASA Planetary Data System (PDS). The data are in
40
41 the Huygens SSP archive maintained on the PDS Atmospheres Node at New Mexico State
42
43 University (presently,
44
45 http://atmos.pds.nasa.gov/data_and_services/atmospheres_data/Huygens/SSP.html) and are
46
47 mirrored on the European Space Agency Planetary Science Archive (PSA) . The data (filename
48
49 SSP_APIV_123456_0_R_ATMOS.TAB) comprise a tabulation of sample times relative to the
50
51 spacecraft reference T0 (the firing of the parachute mortar at the end of the hypersonic entry
52
53 into the atmosphere), an instrument mode flag and record number, and the two times for
54
55
56
57
58
59
60
61
62
63
64
65

1
2
3
4
5 propagation of the sound pulse in each direction, expressed in the raw digital counter number,
6
7 and as a time in milliseconds. Documentation of the data is in the PDS data label file
8
9

10 SSP_APIV_123456_0_R_ATMOS.LBL and the calibration file SSP_CAL.ASC.
11
12

13
14 The latter file notes that the distance between the two transducer faces is 0.1289m, and that
15
16 the digital counter number refers to a 4 MHz clock. As discussed in the text above and in
17
18 Hagermann et al. (2007), there is a ~ 3.7 μs offset to account for the propagation out of and into
19
20 the transducers.
21
22
23
24
25
26
27
28
29
30
31
32
33
34
35

36 < Figure 4 >
37
38
39
40
41

42 Figure 4 shows the recorded API-V dataset taken during Huygens descent. Although API-V was
43
44 switched on only 600 s after initial parachute deployment, the upper atmosphere was too
45
46 tenuous for sufficient atmosphere–sensor coupling and the first successful measurement
47
48 occurred at an altitude of just above 11 km. It can be seen that speed of sound decreases with
49
50 altitude, an effect caused mostly by the associated decrease in temperature. There is also a
51
52 spread of approximately 3 ms^{-1} , much larger than the expected absolute accuracy of the
53
54 sensors of 0.3 ms^{-1} based upon the accuracy of measuring the time of flight and the sensor
55
56 separation. This spread of data has been studied by taking the difference between the
57
58
59
60
61
62
63
64
65

1
2
3
4
5
6 measured time of flight and the value expected for pure nitrogen for all measurements taken
7
8 below 6 km. A random number of peaks is seen during each measurement instead of simply
9
10 missing fewer as the pressure increases. The effect is much reduced on the surface with a
11
12 spread of less than 1 ms^{-1} . Turbulent eddies passing between the sensors during descent might
13
14 have caused a seemingly random change of the scattering properties of the gas, creating this
15
16 effect. This means that each data point can be considered a lower limit on the speed of sound
17
18 with a relative resolution better than 7.5 cm s^{-1} based on the $0.25 \text{ }\mu\text{s}$ sampling rate; but the
19
20 absolute speed of sound could be higher by integer multiples of $\sim 30 \text{ cm s}^{-1}$, based on the 1-
21
22 MHz pulse frequency.
23
24
25
26
27
28
29
30
31

32 3.1 Descent Timeouts and Spurious Early Triggers

33
34
35 In order to obtain a high altitude resolution, e.g. to characterize the planetary boundary layer,
36
37 measurements are made once every second. Although it was only expected that the acoustic
38
39 impedance of the atmosphere would become large enough to reliably detect the transmitted
40
41 pulse towards the end of descent (when the atmosphere would be about 1000 times denser
42
43 than at the start) measurements began at the beginning of descent.
44
45
46
47
48

49
50 A small variation in the actual value of the timeout clock timer is presumably related to
51
52 parametric drift in the timer components : the SSP electronics temperatures (e.g. Leese et al.,
53
54 2012) show a time history very similar to the envelope of the timeouts, with a small increase
55
56 from the beginning until about 3000s, and a slow decline thereafter. The expected timeouts
57
58 were observed through time 1571s, when T1 triggers early, and then more frequently through
59
60
61
62
63
64
65

1
2
3
4
5 ~1844s, when T2 also triggers early. Early triggers are then seen, often in bursts, on both
6
7 channels and in fact more often on T2, until at about 4700s they cease and timeouts resume
8
9 consistently.

10
11
12
13
14 It is tempting to associate these anomalous early triggers with the cause of noise seen on the
15
16
17
18
19
20
21
22
23
24
25
26
27
28
29
30
31
32
33
34
35
36
37
38
39
40
41
42
43
44
45
46
47
48
49
50
51
52
53
54
55
56
57
58
59
60
61
62
63
64
65
It is tempting to associate these anomalous early triggers with the cause of noise seen on the
sonder instrument which we know to be due to the operation of a high speed pump on the
Aerosol Collector/Pyrolyzer instrument (see the pump current and speed history in
housekeeping data archived at
http://atmos.nmsu.edu/PDS/data/hpacp_0001/DATA/ACP_PUMP_V1_0.TAB). This fan
operated at around 25000 rpm from 1500s until 3500s, and 4650-5310s. Thus the
correspondence of the API-V triggers is far from complete and another explanation must be
sought for at least some of the triggers. It seems likely that some kind of turbulence or
aeroacoustic effect may have been responsible. Most curiously, when the instrument appears
to be operating nominally in the lower atmosphere (where the dense gas allows good coupling
and thus a strong signal) T1 again triggers early at 7767s (at about 5km altitude), then again at
7870s, and with increasing frequency through ~8000s where it triggers most of the time until
landing at 8870s.

Some support for an aerodynamic explanation derives from the fact that no early triggers
occurred after landing. Furthermore, the motions of the probe were recorded by
accelerometers and tilt sensors (e.g. Lorenz et al., 2007) which documented that the probe was
buffeted significantly prior to 5500s, but was fairly quiescent thereafter. Although ground tests
showed that the fairly narrow sound beam between the transducers can be scattered by

1
2
3
4
5 modest airflow (e.g. from a desk fan) which would lead to timeouts, turbulent airflow in the SSP
6
7 cavity seems unlikely to be the cause of early triggers, since flow through the instrument is
8
9 limited by a narrow vent tube, and the ESD grille (figure 3) would further suppress airflow
10
11
12
13
14
15
16
17
18
19
20
21
22
23
24
25
26
27
28
29
30
31
32
33
34
35
36
37
38
39
40
41
42
43
44
45
46
47
48
49
50
51
52
53
54
55
56
57
58
59
60
61
62
63
64
65

modest airflow (e.g. from a desk fan) which would lead to timeouts, turbulent airflow in the SSP cavity seems unlikely to be the cause of early triggers, since flow through the instrument is limited by a narrow vent tube, and the ESD grille (figure 3) would further suppress airflow fluctuations. Perhaps the most likely cause of early triggers is vibrations from structural flexing of the probe due to the turbulent motion in this period.

< Figure 5 >

3.2 Post-Landing Suppression of Propagation

< Figure 6 >

< Figure 7 >

The post-landing environment of the Huygens probe was very quiescent after the first ~6 seconds when there was some bouncing and skidding (Bettanini et al., 2007; Schroeder et al., 2012). The orientation of the probe changed very slightly, with a tilt of ~0.2 degrees occurring over 72 minutes (Karkoschka et al., 2007). The camera observed no other changes, apart from a possible methane dewdrop forming on the camera baffle and falling through the field of view (Karkoschka and Tomasko, 2009) - this was observed on Image #897 which was acquired at

1
2
3
4
5
6 T0+10,423s, i.e. 1553s after landing. Additionally, material either inside or immediately
7
8 adjacent to the heated inlet of the GCMS instrument progressively warmed up after landing
9
10 (Lorenz et al., 2006) evolved methane, and later ethane and some other compounds after
11
12 landing (Niemann et al., 2005, 2010). The thermal interactions of the warm - but well-insulated
13
14 and therefore cold-skinned - probe with the surface environment are discussed in Lorenz
15
16
17
18 (2006).
19
20
21
22
23
24

25 Since no major temperature changes occurred, and no major change in position, some change
26
27 in the material around or between the transducers seems to have been responsible for the
28
29 drop in received signals. One hypothesis speculatively advanced in a thesis by Rosenberg (2007)
30
31 was that liquid from the damp subsurface seeped into the cavity made by the probe and
32
33 reduced the atmospheric coupling between the transducers by allowing some of the pulse
34
35 energy to propagate into the liquid and surface material. This scenario could be considered
36
37 under the paradigm that the probe penetrated into the ground, decelerating over a distance of
38
39 around 15cm (e.g. Zarnecki et al., 2005). However, understanding of the probe post-impact
40
41 motion has since improved (Schroeder et al., 2012), concluding that the probe bounced or
42
43 skidded out of this impact depression. There is evidence that the probe was left sitting on the
44
45 surface, rather than having penetrated into it (from the camera geometry, Karkoschka et al.,
46
47 2007, and from the multipath interference pattern observed in the Huygens radio signal, Perez-
48
49 Ayucar et al., 2006). Thus a liquid intrusion scenario seems unlikely.
50
51
52
53
54
55
56
57
58
59
60
61
62
63
64
65

1
2
3
4
5
6 On the other hand, the introduction of heavier gases into the SSP cavity between the
7
8 transducers may have dramatically reduced the pulse strength. With small amounts of gas,
9
10 the sound speed would not be significantly affected, yet the attenuation at 1 MHz could be
11
12 substantially increased, as we note in the next section. It is seen in figure 4 that the post-
13
14 impact propagation times decrease slowly, as would be expected from either warming, or a
15
16 decrease in the relative molecular weight (due to an increasing methane concentration).
17
18
19 However, even assuming the temperature evolution of the instrument (see later) to be
20
21 representative of the acoustic cavity, the interpretation of the post-impact sound speed is not
22
23 unique, since higher molecular weight gases may have partially offset the methane abundance.
24
25
26
27
28
29
30
31
32

33 4. Temperature Environment and Candidate Gas Evolution

34
35
36
37
38
39

40 If we hypothesize that the nondetection of pulses post-landing is due to the introduction of an
41
42 attenuating gas into the SSP cavity, then we can use the descent data as a proxy calibration.
43
44 Specifically, for the absorber to cause the loss of signal, it must introduce an attenuation
45
46 equivalent to the difference in transmission between the unperturbed atmosphere at the
47
48 surface and the atmosphere at the altitude where a similarly low pulse detection rate was
49
50 encountered. Specifically, since the detection rate was near-zero at ~10km altitude, the
51
52 surface absorber must have attenuated the signal by a factor of $\sim(\rho_{10}c_{10}/\rho_0c_0)^2$ or
53
54 $[(3.5*184)/(5.4*194)]^2 = 0.37$, 1 neper (np) or 4.3dB. Thus the localized atmosphere in the SSP
55
56
57
58
59
60
61
62
63
64
65

1
2
3
4
5 cavity has an attenuation coefficient α of $4.3/0.12 \sim 40$ dB/m or ~ 8 np/m : it is probable that
6
7
8 this aggregate attenuation is the result of the absorption by several different gas species
9
10
11 together, each at a modest concentration.

12
13
14 Dain and Lueptow (2001) examine the attenuation in methane-air mixtures, showing that the
15
16
17 attenuation ($\alpha\lambda$) at 600kHz/bar is substantially influenced by molecular relaxation of methane,
18
19
20 having $\alpha\lambda \sim 0.01$ for high methane concentrations at 297K. For the wavelength of the Titan
21
22
23 experiment with $c \sim 200$ m/s, $\lambda \sim 0.2$ mm and thus $\alpha \sim 50$ np/m for pure methane. The methane
24
25
26 concentration was measured (Niemann et al., 2005) to be $\sim 5\%$ in the free atmosphere (where
27
28
29 of course the pulses were transmitted successfully), but it could have risen slightly in the SSP
30
31
32 cavity. Heavier gases which were essentially absent in the free atmosphere but which may
33
34
35 have accumulated in the warming cavity seem a more likely candidate to provide the
36
37
38 incremental attenuation. Ethane is a strong candidate (see later) but there are several others
39
40
41 (see figures 8 and 9) and it will not be possible to discriminate their contributions since
42
43
44 measurements at only one frequency were made.

45
46
47 Martinsson and Delsing (2002) give measurements of the attenuation of (pure) ethane at
48
49
50 600kHz/bar (i.e. the condition of the 1MHz measurement at 1.5 bar) of 30-40 neper/m. The
51
52
53 corresponding attenuation of Carbon monoxide was ~ 10 neper/m. Holmes et al. (1964) obtain
54
55
56 a similar value for ethane, and find propane to have an attenuation about a factor of 2 lower.

57
58
59 All these data are at room temperature.
60
61
62
63
64
65

1
2
3
4
5 < Figure 8 >
6
7

8
9 < Figure 9 >
10
11
12
13
14

15
16 The quantitative interpretation of the Huygens measurement really requires low-temperature
17
18 attenuation measurements which are not, as far as the authors are aware, available. The
19
20 actual gas mixture that formed in the acoustic cavity on Huygens cannot in any case be uniquely
21
22 determined : our only intent here is to show that methane, ethane and carbon dioxide
23
24 (compounds known to be present on the Titan surface) and other organics (like ethylene and
25
26 many others) can provide significant acoustic absorption at the frequencies discussed.
27
28
29
30
31

32
33
34
35
36 Niemann et al. (2005; 2010) show that the GCMS instrument detected several species after
37
38 landing (see figure 10). Note that there is no expectation of an exact correspondence between
39
40 the GCMS readings and the gas abundances in the SSP cavity since the thermal histories of
41
42 whatever material was jammed into the heated GCMS inlet and the possibility of evaporation
43
44 of dampness around it and its diffusion into the gas sampling tubes may have been quite
45
46 different from the warming of any material scraped into the SSP cavity or warmed underneath
47
48 the probe. However, the overall timeline is probably representative - e.g. figure 11 shows the
49
50 warming of the interior of the top hat, and the corresponding dew point of the ethane partial
51
52 pressure measured by GCMS (which should be seen only as representative, since the
53
54
55
56
57
58
59
60
61
62
63
64
65

1
2
3
4
5 temperature evolutions of GCMS and SSP would not have been identical, and the ethane vapor
6
7
8 pressure may have been influenced by other solutes in the damp ground).
9

10
11 The saturation vapor pressure of pure ethane is very small (equivalent to a mixing ratio of
12
13 about 30ppm at Titan's surface temperature of 94K) but rises steeply with temperature. Should
14
15 surface material damp with ethane have warmed to 120-140K, the saturation mixing ratio
16
17 would increase to 0.2-2%. The GCMS data show that several other compounds rose in detected
18
19 abundance over an hour or so after landing. Benzene and cyanogen were detected, and so it
20
21 seems likely that a rich cocktail of hydrocarbons and nitriles (and, indeed, CO₂, a well-known
22
23 acoustic absorber) may have similarly accumulated in the top hat cavity.
24
25
26
27
28
29
30
31
32
33

34 Leese et al. (2012) noted that during API-V Specific to Experiment Test on the flight model
35
36 probe, which involved using a purpose built Top Hat non-flight cover to introduce several
37
38 different gases and flush through the Top Hat cavity for each, carbon dioxide produced
39
40 timeouts (i.e. no signal detected) for very low concentrations in nitrogen due to high acoustic
41
42 absorption. In addition to this well-known effect of the pure gas, Garry (1996) noted in ground
43
44 tests of the API-V system that an order of magnitude drop in signal was encountered when
45
46 purging a test cavity with nitrogen after making measurements in ethane or methane. This
47
48 transient attenuation due to nitrogen/methane or nitrogen/ethane mixtures could not be
49
50 characterized in detail, unfortunately, since no means was available to measure the changing
51
52 composition. Thus we call attention to the need for quantitative acoustic absorption
53
54 measurements of nitrogen mixtures with other gases, at temperatures of around 100K.
55
56
57
58
59
60
61
62
63
64
65

1
2
3
4
5
6
7
8
9 < Figure 10 >

10
11
12 < Figure 11 >

13
14
15
16
17
18
19 The statistical behavior of the lost pulses is interesting, in that bursts of pulses appear to break
20 through above the detection threshold - e.g. at 9800-9900s, these bursts are 5-10s long,
21 whereas later, at 10000s (see figure 12) the bursts are more like 20s. Furthermore, when
22 propagation is successful in one direction (e.g. T1) it is often also successful in the other,
23 suggesting a common factor. One possibility might be that the gas supply and/or removal is
24 discretized somehow, e.g. bubbles of gas released from the subsurface like a plopping mudpot.

25
26
27
28
29
30
31
32
33
34
35 There is unfortunately little data to constrain such speculation, although any subsurface
36 phenomena were evidently too weak to cause any disturbance measurable by the sensitive
37 accelerometers and tiltmeters on the probe.
38
39
40
41
42
43
44
45
46

47 < Figure 12 >

48 49 50 51 52 53 54 5. Conclusions

55
56
57 The speed-of-sound instrument, whose principal intended role on the payload was to measure
58 the properties of Titan's seas, nonetheless provided some information during descent and after
59
60
61
62
63
64
65

1
2
3
4
5 landing, and suggests that sound propagation was suppressed about 20 minutes after
6
7
8 touchdown.
9

10
11 Clearly, using the function of a threshold detector in this way is not an ideal attenuation
12
13 measurement, having a very modest dynamic range. Nonetheless, the most plausible
14
15 interpretation of the cessation of signals post-landing is the evolution of absorbing vapors from
16
17 the surface. This independent detection of volatiles reinforces the notion that the surface
18
19 materials at the landing site were 'damp', and underscores that unexpected results can be
20
21 obtained from acoustic instrumentation. We may recall the words of Charlotte Bronte "Silence
22
23 is of different kinds, and breathes different meanings."
24
25
26
27
28
29

30
31 One lesson is that the interpretation of a notionally-simple instrument in an unknown
32
33 environment was rather complex. A housekeeping measurement of signal strength, even on a
34
35 small subset of the measurements, would have greatly assisted interpretation. More
36
37 ambitiously, the ability to measure at a range of frequencies - to conduct acoustic absorption
38
39 spectroscopy - might permit identification of the absorbing gases. Of course on future Titan
40
41 missions any such augmented capabilities would be in competition with a range of other
42
43 scientific experiments and so the richness and significance of findings that might result must be
44
45 traded off against the resource requirements and the opportunity costs of other types of
46
47 instrumentation.
48
49
50
51
52
53
54
55
56
57

58 6. Acknowledgements

59
60
61
62
63
64
65

1
2
3
4
5 Cassini-Huygens is a joint endeavour of NASA, ESA and ASI. The results reported here were
6
7
8 made possible by the efforts of many colleagues on the Huygens team. RL acknowledges the
9
10 support of the Cassini project at the Jet Propulsion Laboratory, via NASA grant NNX13AH14G.
11
12
13 The lead author acknowledges useful discussions on acoustics with Juan Arvelo of APL and Tim
14
15
16 Leighton of the University of Southampton.
17
18
19
20
21
22
23
24
25
26
27
28
29
30
31
32
33
34
35
36
37
38
39
40
41
42
43
44
45
46
47
48
49
50
51
52
53
54
55
56
57
58
59
60
61
62
63
64
65

1
2
3
4
5
6
7
8
9
10
11
12
13
14
15
16
17
18
19
20
21
22
23
24
25
26
27
28
29
30
31
32
33
34
35
36
37
38
39
40
41
42
43
44
45
46
47
48
49
50
51
52
53
54
55
56
57
58
59
60
61
62
63
64
65

References

Bettanini, C., Zaccariotto, M., Angrilli, F., 2008. Analysis of the HASI accelerometers data measured during the impact phase of the Huygens probe on the surface of Titan by means of a simulation with a finite element model. *Planetary and Space Science* 56, 715–727.

Dain, Y. and R. M. Lueptow, 2001. Acoustic Attenuation in a three-gas mixture: Results, *J. Acoustical Society of America*, 110, 2974-2979

Ejakov, S. G. Acoustic attenuation in gas mixtures with nitrogen : Experimental data and calculations, *J. Acoustical Society of America*, 113, 1871-1879

Garry, J.R.C., 1996. Surveying Titan Acoustically. MSc Thesis, University of Kent at Canterbury, Canterbury. (Garry, J.R.C., Kent, M.Sc., 1996, C3 46-9855).

Hagermann, A., P.D. Rosenberg, M.C. Towner, J.R.C. Garry, H. Svedhem, M.R. Leese, B. Hathi, R.D. Lorenz, J. C. Zarnecki, 2007. Speed of sound measurements and the methane abundance in Titan's atmosphere, *Icarus*, 189, 538-543

Hanford, A. D. and L. N. Long, 2009. The direct simulation of acoustics on Earth, Mars and Titan, *J. Acoustical Society of America*, 125, 640-650

Holmes, R., G. R. Jones and N. Pusat, 1964. Vibrational Relaxation in Propane, Propylene and Ethane, *Journal of Chemical Physics*, 41, 2512-2516

1
2
3
4
5 Karkoschka, E., Tomasko, M.G., Doose, L.R., See, C., McFarlane, E.A., Schroeder, S.E., Rizk, B.,
6
7
8 2007. DISR imaging and the geometry of the descent of Huygens. *Planetary and Space Science*
9
10 55, 1896–1935.

11
12
13
14 Karkoschka, E., Tomasko, M.G 2009. Rain and dewdrops on titan based on in situ imaging,
15
16
17 *Icarus*, 199, 442-448

18
19
20
21
22
23 Leese, M. R., R. D. Lorenz, B. Hathi and J. C. Zarnecki, 2012. The Huygens Surface Science
24
25
26 Package (SSP): Flight Performance Review and Lessons Learned, *Planetary and Space Science*,
27
28
29 70, 28-45

30
31
32 Leighton, T. G. and White, P. R.,2004. The Sound of Titan - a role for acoustics in space
33
34
35 exploration, *Acoust. Bull.* 16-23

36
37
38 Leighton, T.G. and Petculescu, A. 2009. The sound of music and voices in space, *Acoustics*
39
40
41 Today, 5, 17-29

42
43
44 Lorenz, R. D. 1994. Exploring the Surface of Titan, Ph.D. Thesis, University of Kent at Canterbury

45
46
47
48 Lorenz, R. D., 2006. Thermal Interaction of the Huygens Probe with the Titan Environment :
49
50
51 Surface Windspeed Constraint, *Icarus*, 182, 559-566

52
53
54 Lorenz, R. D., H. Niemann, D. Harpold, J. Zarnecki, Titan's Damp Ground : Constraints on Titan
55
56
57 Surface Thermal Properties from the Temperature Evolution of the Huygens GCMS inlet, 2006.
58
59
60 *Meteoritics and Planetary Science.* 41, 1405-1414

1
2
3
4
5 Lorenz, R. D., J. C. Zarnecki, M. C. Towner, M. R. Leese, A. J. Ball, B. Hathi, A. Hagermann, N. A.

6
7
8 L. Ghafoor, 2007. Descent Motions of the Huygens Probe as Measured by the Surface Science
9
10 Package (SSP) : Turbulent Evidence for A Cloud Layer, Planetary and Space Science, 55, 1936-
11
12 1948
13

14
15
16 Lorenz, R. D., 2007. Titan Atmosphere Profiles from Huygens Engineering (Temperature and
17
18 Acceleration) Sensors, Planetary and Space Science, 55, 1949-1958
19
20

21
22
23 Martinsson, P.-E., and J. Delsing, 2002. Ultrasonic Measurements of Molecular Relaxation in
24
25 Ethane and Carbon Monoxide, pp.511-515 in Proceedings, 2002 IEEE Ultrasonics Symposium.
26
27

28
29 Niemann, H.B., Atreya, S.K., Bauer, S.J., Carignan, G.R., Demick, J.E., Frost, R.L., Gautier, D.,
30
31 Haberman, J.A., Harpold, D.N., Hunten, D.M., Israel, G., Lunine, J.I., Kasprzak, W.T., Owen, T.C.,
32
33 Paulkovich, M., Raulin, F., Raaen, E., Way, S.H., 2005. The abundances of constituents of Titan's
34
35 atmosphere from the GCMS instrument on the Huygens probe. Nature 438, 779–784.
36
37

38
39
40 Niemann, H. B., S. K. Atreya, J. E. Demick, D. Gautier, J. A. Haberman, D. N. Harpold, W. T.
41
42 Kasprzak, J. I. Lunine, T. C. Owen, and F. Raulin, 2010. Composition of Titan's lower atmosphere
43
44 and simple surface volatiles as measured by the Cassini-Huygens probe gas chromatograph
45
46 mass spectrometer experiment, Journal of Geophysical Research, 115, E12006,
47
48
49
50
51 doi:10.1029/2010JE003659
52

53
54 Pérez-Ayúcar M., Lorenz R. D., Flourey N., Prieto R., Lebreton J.-P., 2006. Surface Properties of
55
56 Titan from Post-Landing Reflections of the Huygens Radio Signal, JGR – Planets, 111, E07001,
57
58
59
60
61
62
63
64
65
66
67
68
69
70
71
72
73
74
75
76
77
78
79
80
81
82
83
84
85
86
87
88
89
90
91
92
93
94
95
96
97
98
99
100
doi:10.1029/2005JE002613

1
2
3
4
5
6 Petculescu, A., B. Hall, R. Fraenzle, S. Phillips, R. M. Lueptow, 2006. A prototype acoustic gas
7
8 sensor based on attenuation, J. Acoustical Society of America, 120, 1779-1782
9

10
11 Petculescu, A. and P. Achi, 2012. A model for the vertical sound speed and absorption profiles
12
13 in Titan's atmosphere based on Cassini-Huygens data, J. Acoustical Society of America, 131,
14
15 3671-3679
16
17

18
19 Petculescu, A. and R. M. Lueptow, 2007. Atmospheric acoustics of Titan, Mars, Venus, and
20
21 Earth, Icarus, 186, 413-319
22
23

24
25 Rosenberg, P.D., 2007. Huygens' Measurements of the Speed of Sound on Titan. PhD Thesis,
26
27 The Open University, Milton Keynes. (An EThOS/ BL Reference number for the 2008 thesis by
28
29 Rosenberg, P.D. is DXN116951)
30
31
32

33
34 Schroeder, S. E., E. Karkoschka and R. D. Lorenz, 2012. Bouncing on Titan : Motion of the
35
36 Huygens Probe in the seconds after landing, Planetary and Space Science, 73, 327-340
37
38

39
40 Svedhem, H., Lebreton, J.-P., Zarnecki, J.C., Hathi, B., 2004. Using speed of sound
41
42 measurements to constrain the Huygens probe descent profile. ESA SP-544, 221-228.
43
44
45
46
47
48
49
50
51
52
53
54
55
56
57
58
59
60
61
62
63
64
65

1
2
3
4
5
6
7
8
9 Towner, M. C., J.R.C. Garry, R.D. Lorenz, B. Hathi, A. Hagermann, H. Svedhem, B.C. Clark, M.R.

10
11 Leese, J.C. Zarnecki, 2006. Physical properties of the Huygens landing site from the Surface

12
13 Science Package Acoustic Properties sensor (API S), Icarus, 185, 457-465

14
15
16
17 Zarnecki, J.C., Banaszkiwicz, M., Bannister, M., Boynton, W.V., Challenor, P., Clark, B., Daniell,

18
19 P.M., Delderfield, J., English, M.A., Garry, J.R.C., Geake, J.E., Green, S.F., Hathi, B., Jaroslowski,

20
21 S., Leese, M.R., Lorenz, R.D., McDonnell, J.A.M., Merryweather-Clarke, N., Mill, C.S., Miller, R.J.,

22
23
24
25 Newton, G., Parker, D.J., Svedhem, H., Wright, M.J., 1997. The Huygens Surface Science

26
27 Package. In: Wilson, A. (Ed.), Huygens: Science, Payload and Mission. ESA SP-1177. ESA

28
29 Publications Division, Noordwijk, pp. 177–195.

30
31
32
33 Zarnecki, J.C., Leese, M.R., Garry, J.R.C., Ghafoor, N., Hathi, B., 2002. Huygens' Surface Science

34
35 Package. Space Sci. Rev., 104, 593–611.

36
37
38
39 Zarnecki, J.C., Leese, M.R., Hathi, B., Ball, A.J., Hagermann, A., Towner, M.C., Lorenz, R.D.,

40
41 McDonnell, J.A.M., Green, S.F., Patel, M.R., Ringrose, T.J., Rosenberg, P.D., Atkinson, K.R.,

42
43 Paton, M.D., Banaszkiwicz, M., Clark, B.C., Ferri, F., Fulchignoni, M., Ghafoor, N.A.L., Kargl, G.,

44
45
46
47 Svedhem, H., Delderfield, J., Grande, M., Parker, D.J., Challenor, P.G., Geake, J.E., 2005. A soft

48
49 solid surface on Titan at the Huygens landing site as measured by the Surface Science Package

50
51 (SSP). Nature 438 (7069), 792795.

Figure Captions

Figure 1. Location of the SSP API-V sensors on the underside of the Huygens probe, with the anti-static screen shown displaced downwards for clarity.

Figure 2 . View of the SSP 'Top Hat' structure with the grill removed. The metallic boxes at top and bottom are the API-V speed of sound transducer housings (the circular transducer surface is just visible on the right one). The penetrometer is visible at left (note also the grounding strap) and the acoustic sounder at lower right.

Figure 3. The metal grill shown in position on the front of the SSP Top Hat. Most photographs of the probe show the instrumentation with the grill removed, but it is important in understanding the possible influences on the acoustic instrumentation.

Figure 4. The API-V data against mission time. The 'good' propagation times (A) measured during the lower part of descent have been analyzed in detail by Hagermann et al. (2007). Surface measurements (B) are discussed in the present paper. For most of the descent, the receive pulse threshold was not crossed and the counter timed out, forming two clouds of points (C, D) - the timeout was different for the two propagation directions. A spurious set of early triggers (E) are present and are discussed in the text and may be related to noise from the Aerosol Collector Pyrolyzer (ACP) pump.

Figure 5. Statistics of T2 propagation times in 200s blocks leading up to landing (dataset A in figure 4). Initially (6650s, about 14km) there are no received pulses and only timeouts at

1
2
3
4
5
6 ~0.78ms are present. As the probe descends into denser air, propagated pulses begin to appear
7
8 correctly at ~0.7ms and progressively dominate, with almost no timeouts present after ~8000s,
9
10
11 until the last 1km of descent. Why this should occur is not clear.

12
13
14 Figure 6. Statistics of propagation times (x-axis, milliseconds) in 200-second blocks of data
15
16 after landing (dataset B in figure 4). The right-hand peaks (>0.72 ms) correspond to timeouts,
17
18 the left hand peak to valid pulse receipt. Data start 30s after the impact at 8870s - it is known
19
20 that the probe was still moving for a few seconds after contact. Initially (8900-9100s) there are
21
22 no clean pulses, perhaps as a result of material adhering to the transducers. Over 9100-9500s a
23
24 good strong signal builds up and the proportion of timeouts declines, but then increases again
25
26 over 9500-10300s, with no further clean pulses getting through thereafter. Notice also that
27
28 while at 9100s-9300s the 'good' pulse histogram is sharp indicating clean triggers from a strong
29
30 signal, the histogram for 9700s and thereafter is broader and positively skewed, i.e. with a
31
32 fraction of 'late' triggers. As discussed in Hagermann et al. (2007) this is a signature of a weak
33
34
35
36
37
38
39
40
41
42
43
44
45
46
47
48
49
50
51
52
53
54
55
56
57
58
59
60
61
62
63
64
65
66
67
68
69
70
71
72
73
74
75
76
77
78
79
80
81
82
83
84
85
86
87
88
89
90
91
92
93
94
95
96
97
98
99
100
101
102
103
104
105
106
107
108
109
110
111
112
113
114
115
116
117
118
119
120
121
122
123
124
125
126
127
128
129
130
131
132
133
134
135
136
137
138
139
140
141
142
143
144
145
146
147
148
149
150
151
152
153
154
155
156
157
158
159
160
161
162
163
164
165
166
167
168
169
170
171
172
173
174
175
176
177
178
179
180
181
182
183
184
185
186
187
188
189
190
191
192
193
194
195
196
197
198
199
200
201
202
203
204
205
206
207
208
209
210
211
212
213
214
215
216
217
218
219
220
221
222
223
224
225
226
227
228
229
230
231
232
233
234
235
236
237
238
239
240
241
242
243
244
245
246
247
248
249
250
251
252
253
254
255
256
257
258
259
260
261
262
263
264
265
266
267
268
269
270
271
272
273
274
275
276
277
278
279
280
281
282
283
284
285
286
287
288
289
290
291
292
293
294
295
296
297
298
299
300
301
302
303
304
305
306
307
308
309
310
311
312
313
314
315
316
317
318
319
320
321
322
323
324
325
326
327
328
329
330
331
332
333
334
335
336
337
338
339
340
341
342
343
344
345
346
347
348
349
350
351
352
353
354
355
356
357
358
359
360
361
362
363
364
365
366
367
368
369
370
371
372
373
374
375
376
377
378
379
380
381
382
383
384
385
386
387
388
389
390
391
392
393
394
395
396
397
398
399
400
401
402
403
404
405
406
407
408
409
410
411
412
413
414
415
416
417
418
419
420
421
422
423
424
425
426
427
428
429
430
431
432
433
434
435
436
437
438
439
440
441
442
443
444
445
446
447
448
449
450
451
452
453
454
455
456
457
458
459
460
461
462
463
464
465
466
467
468
469
470
471
472
473
474
475
476
477
478
479
480
481
482
483
484
485
486
487
488
489
490
491
492
493
494
495
496
497
498
499
500
501
502
503
504
505
506
507
508
509
510
511
512
513
514
515
516
517
518
519
520
521
522
523
524
525
526
527
528
529
530
531
532
533
534
535
536
537
538
539
540
541
542
543
544
545
546
547
548
549
550
551
552
553
554
555
556
557
558
559
560
561
562
563
564
565
566
567
568
569
570
571
572
573
574
575
576
577
578
579
580
581
582
583
584
585
586
587
588
589
590
591
592
593
594
595
596
597
598
599
600
601
602
603
604
605
606
607
608
609
610
611
612
613
614
615
616
617
618
619
620
621
622
623
624
625
626
627
628
629
630
631
632
633
634
635
636
637
638
639
640
641
642
643
644
645
646
647
648
649
650
651
652
653
654
655
656
657
658
659
660
661
662
663
664
665
666
667
668
669
670
671
672
673
674
675
676
677
678
679
680
681
682
683
684
685
686
687
688
689
690
691
692
693
694
695
696
697
698
699
700
701
702
703
704
705
706
707
708
709
710
711
712
713
714
715
716
717
718
719
720
721
722
723
724
725
726
727
728
729
730
731
732
733
734
735
736
737
738
739
740
741
742
743
744
745
746
747
748
749
750
751
752
753
754
755
756
757
758
759
760
761
762
763
764
765
766
767
768
769
770
771
772
773
774
775
776
777
778
779
780
781
782
783
784
785
786
787
788
789
790
791
792
793
794
795
796
797
798
799
800
801
802
803
804
805
806
807
808
809
810
811
812
813
814
815
816
817
818
819
820
821
822
823
824
825
826
827
828
829
830
831
832
833
834
835
836
837
838
839
840
841
842
843
844
845
846
847
848
849
850
851
852
853
854
855
856
857
858
859
860
861
862
863
864
865
866
867
868
869
870
871
872
873
874
875
876
877
878
879
880
881
882
883
884
885
886
887
888
889
890
891
892
893
894
895
896
897
898
899
900
901
902
903
904
905
906
907
908
909
910
911
912
913
914
915
916
917
918
919
920
921
922
923
924
925
926
927
928
929
930
931
932
933
934
935
936
937
938
939
940
941
942
943
944
945
946
947
948
949
950
951
952
953
954
955
956
957
958
959
960
961
962
963
964
965
966
967
968
969
970
971
972
973
974
975
976
977
978
979
980
981
982
983
984
985
986
987
988
989
990
991
992
993
994
995
996
997
998
999
1000

Figure 7. 200-sample running mean of the fraction of good pulses (i.e. transit times in the valid range of 0.6 to 0.7 ms) in the two directions (T1, T2) just after landing. In fact the performance jumps rapidly upwards after landing (the 200-sample smoothing limits the gradient, but shows better the quantitative decline in performance after 9500s).

1
2
3
4
5
6 Figure 8. Dimensionless attenuation of several gases mixed with nitrogen. The Huygens API-V
7
8 measurement on the surface corresponds to $f/P=6E5$ Hz/bar, rather close to where the
9
10 ethylene absorption has a peak. Curves extracted from Petelescu et al. (2006) and Dain and
11
12 Lueptow (2001).
13
14

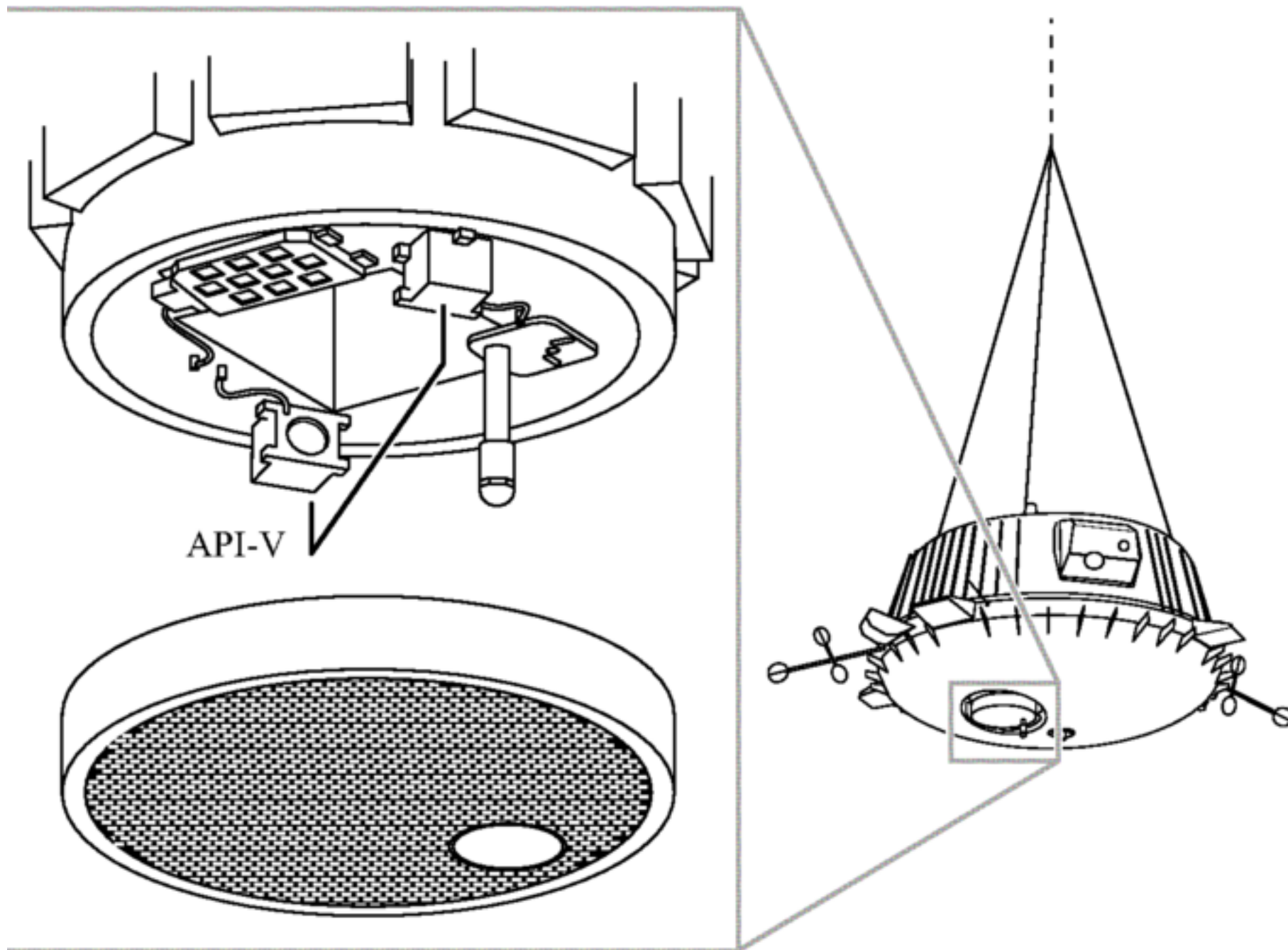
15
16
17 Figure 9. Dimensionless attenuation for several gas mixtures. Note the very strong absorption
18
19 by CO_2 , although this peaks at a frequency an order of magnitude lower than that for ethylene
20
21 (C_2H_4). Curves extracted from Petelescu et al. (2006) and Dain and Lueptow (2001).
22
23
24

25
26 Figure 10. The mixing ratio evolution of some acoustically-absorbing gases sampled by the
27
28 Huygens GCMS (Niemann et al., 2010). The rise post-impact is due to heating of the inlet,
29
30 embedded in the surface material.
31
32

33
34 Figure 11. Temperature evolution of the PERmittivity sensor near the front of the top hat.
35
36 Although formally unrelated, the dew point of the ethane partial pressure indicated by the
37
38 GCMS is also shown, illustrating the broad consistency between the rise of probe-base
39
40 temperatures and the presence of volatiles. The period in which the pulse transit efficiency
41
42 declines to zero is indicated, and corresponds with the rise in volatile abundance.
43
44
45
46
47
48
49
50
51
52
53
54
55
56
57
58
59
60
61
62
63
64
65

1
2
3
4
5
6 Figure 13. Time series of data (essentially a zoom of figure 4) as the overall propagation
7
8 probability was declining on the surface. Valid data tends to appear in bursts in both directions,
9
10 here around 20s long, with T2 tending to fail more often.
11
12
13
14
15
16
17
18
19
20
21
22
23
24
25
26
27
28
29
30
31
32
33
34
35
36
37
38
39
40
41
42
43
44
45
46
47
48
49
50
51
52
53
54
55
56
57
58
59
60
61
62
63
64
65

Figure
[Click here to download high resolution image](#)



Figure

[Click here to download high resolution image](#)



Figure

[Click here to download high resolution image](#)

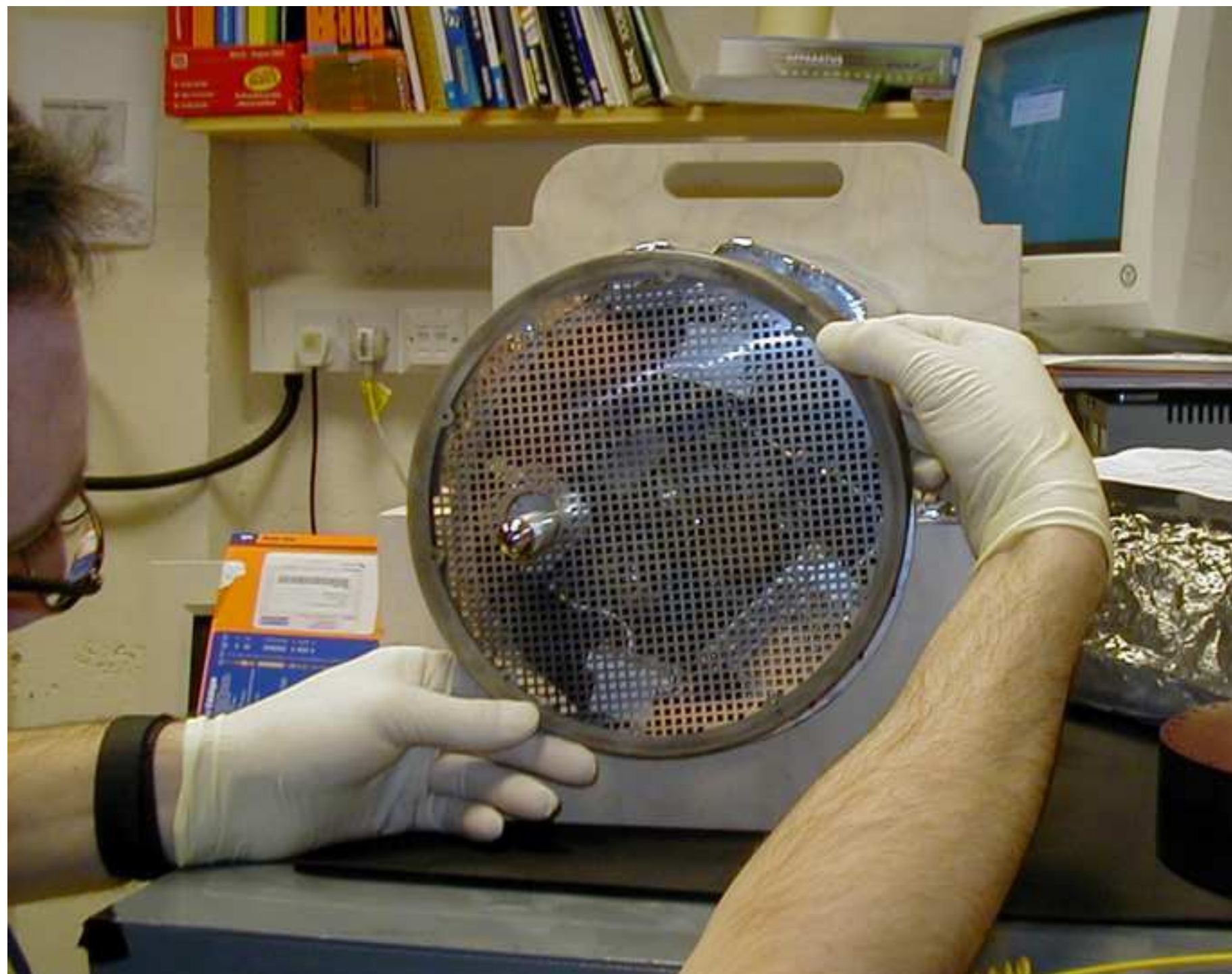
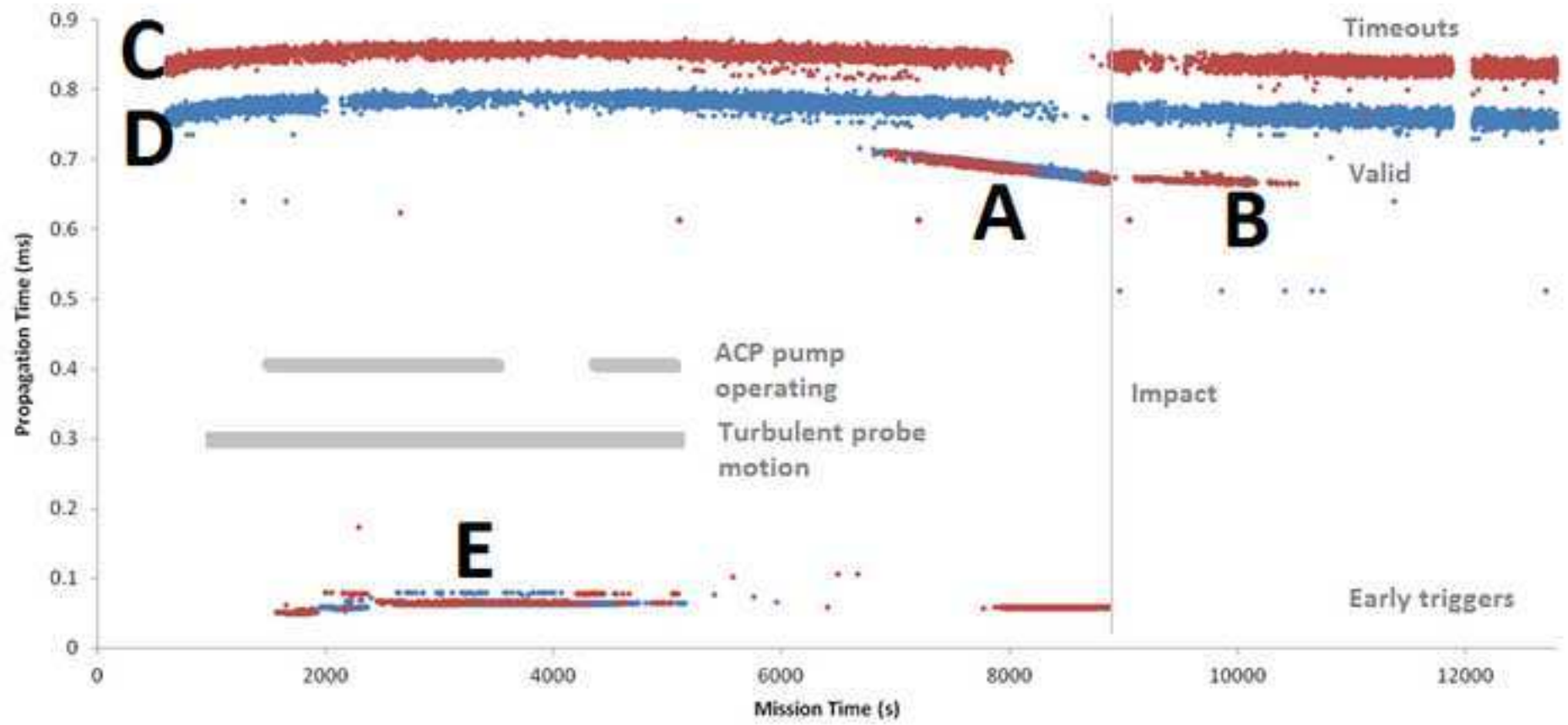
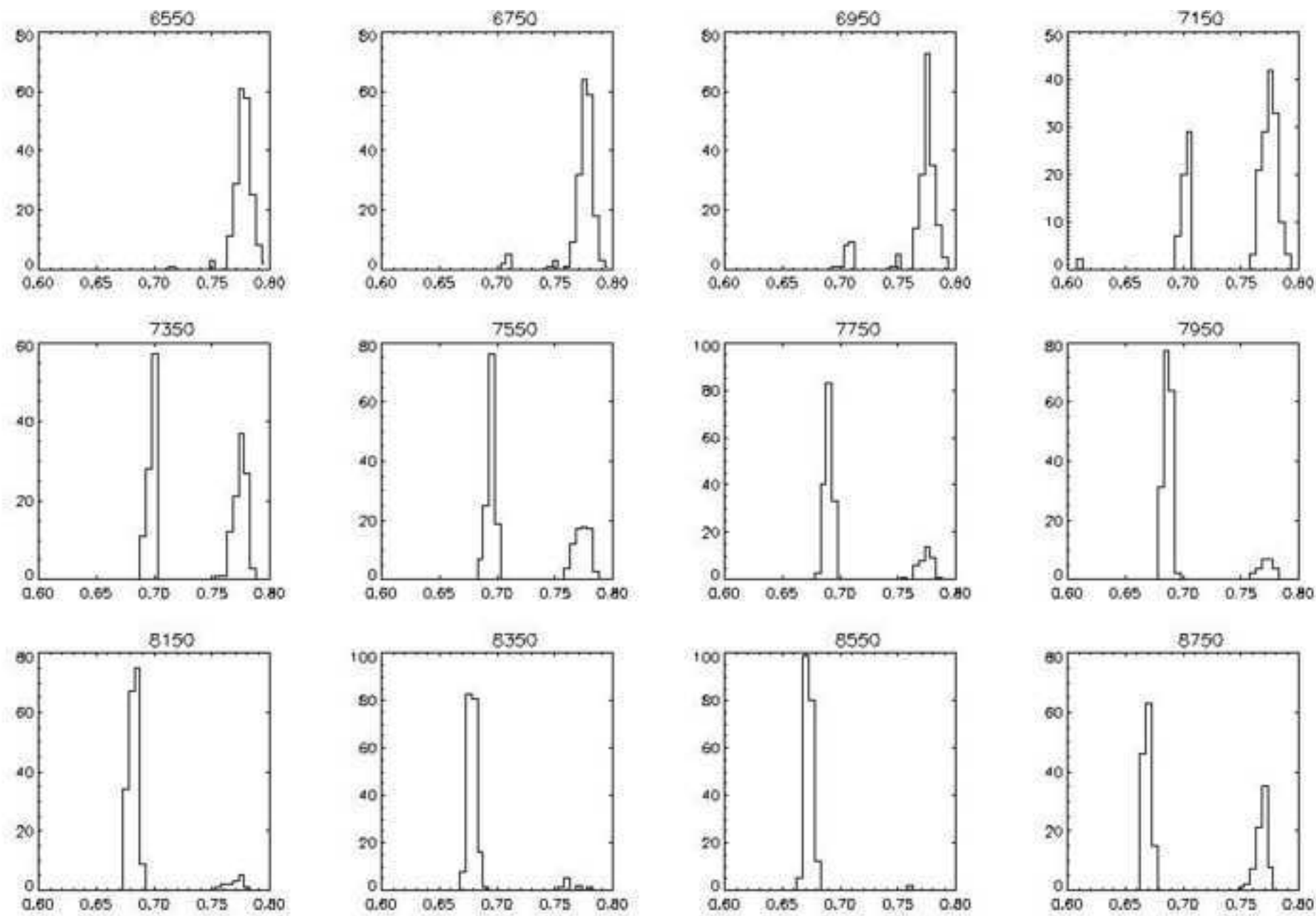


Figure
[Click here to download high resolution image](#)



Figure

[Click here to download high resolution image](#)



Figure

[Click here to download high resolution image](#)

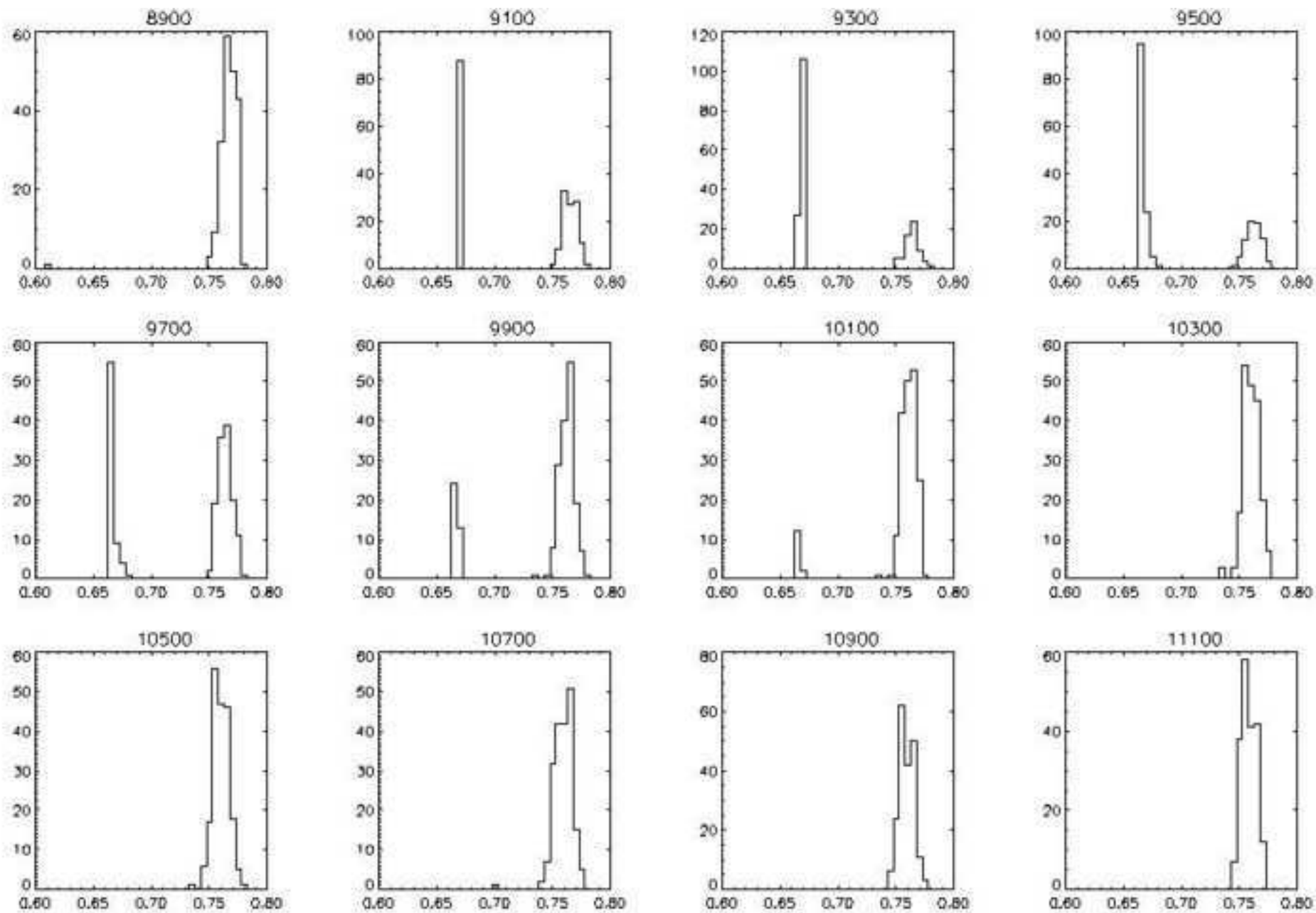


Figure
[Click here to download high resolution image](#)

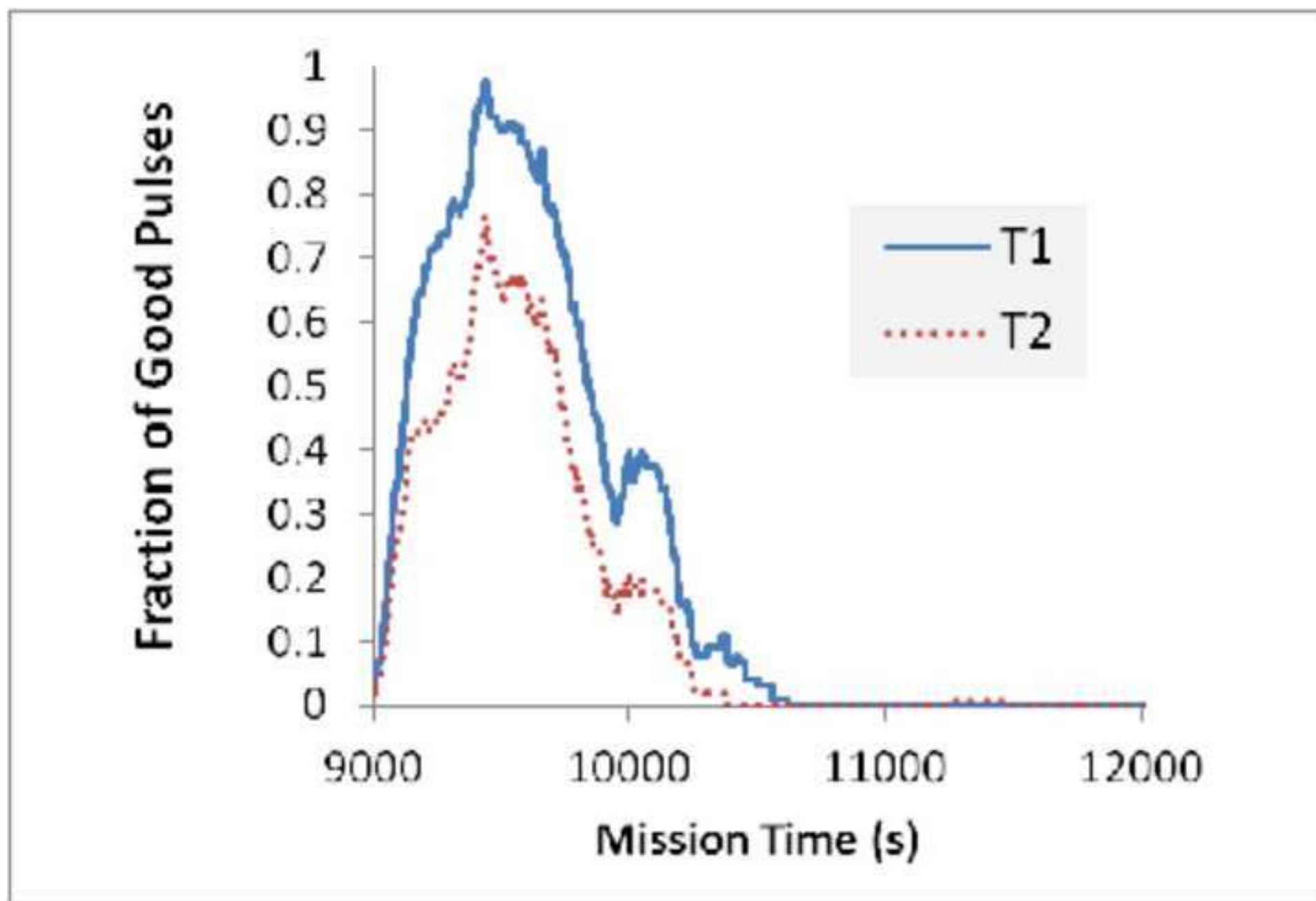


Figure
[Click here to download high resolution image](#)

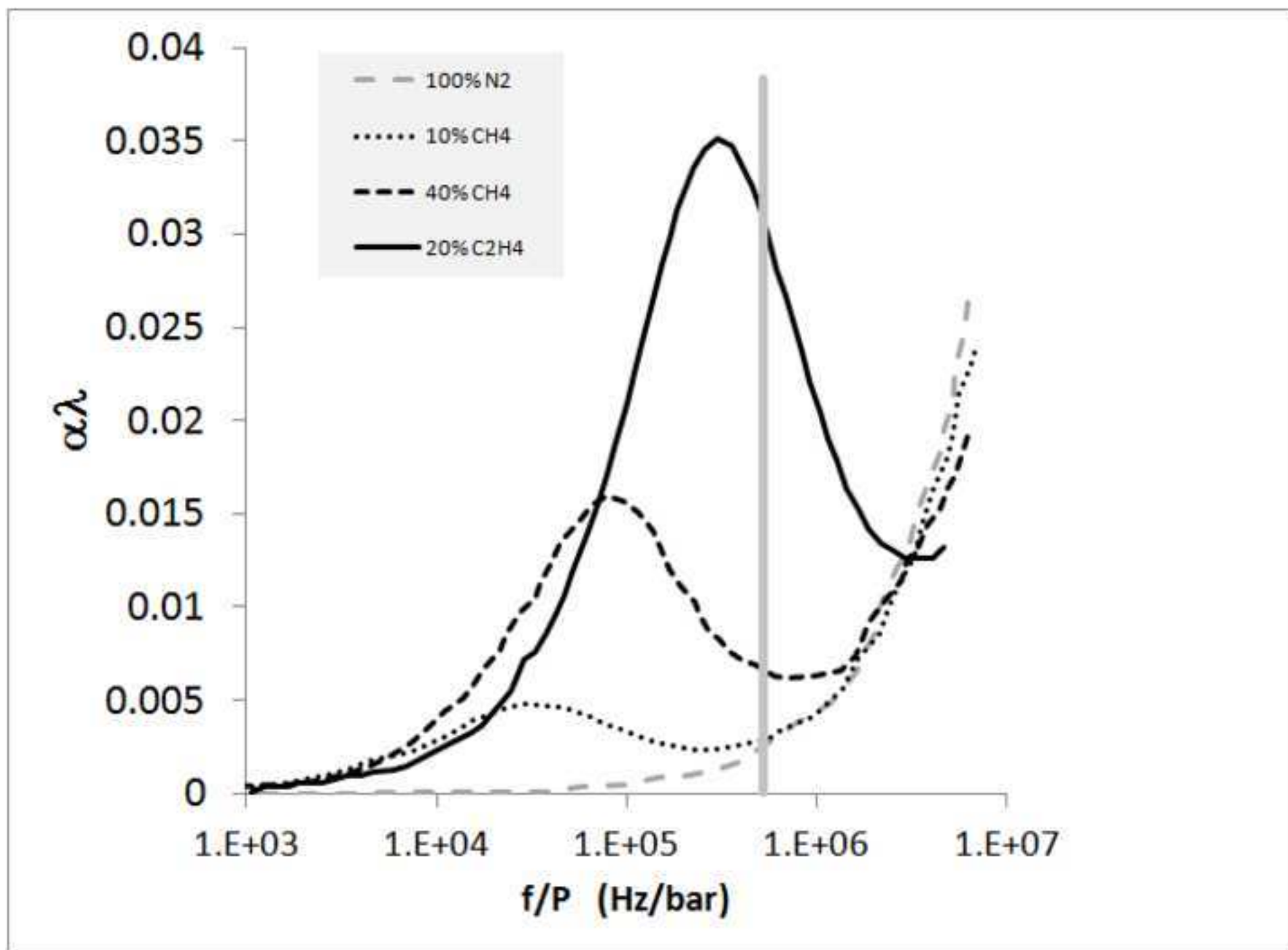
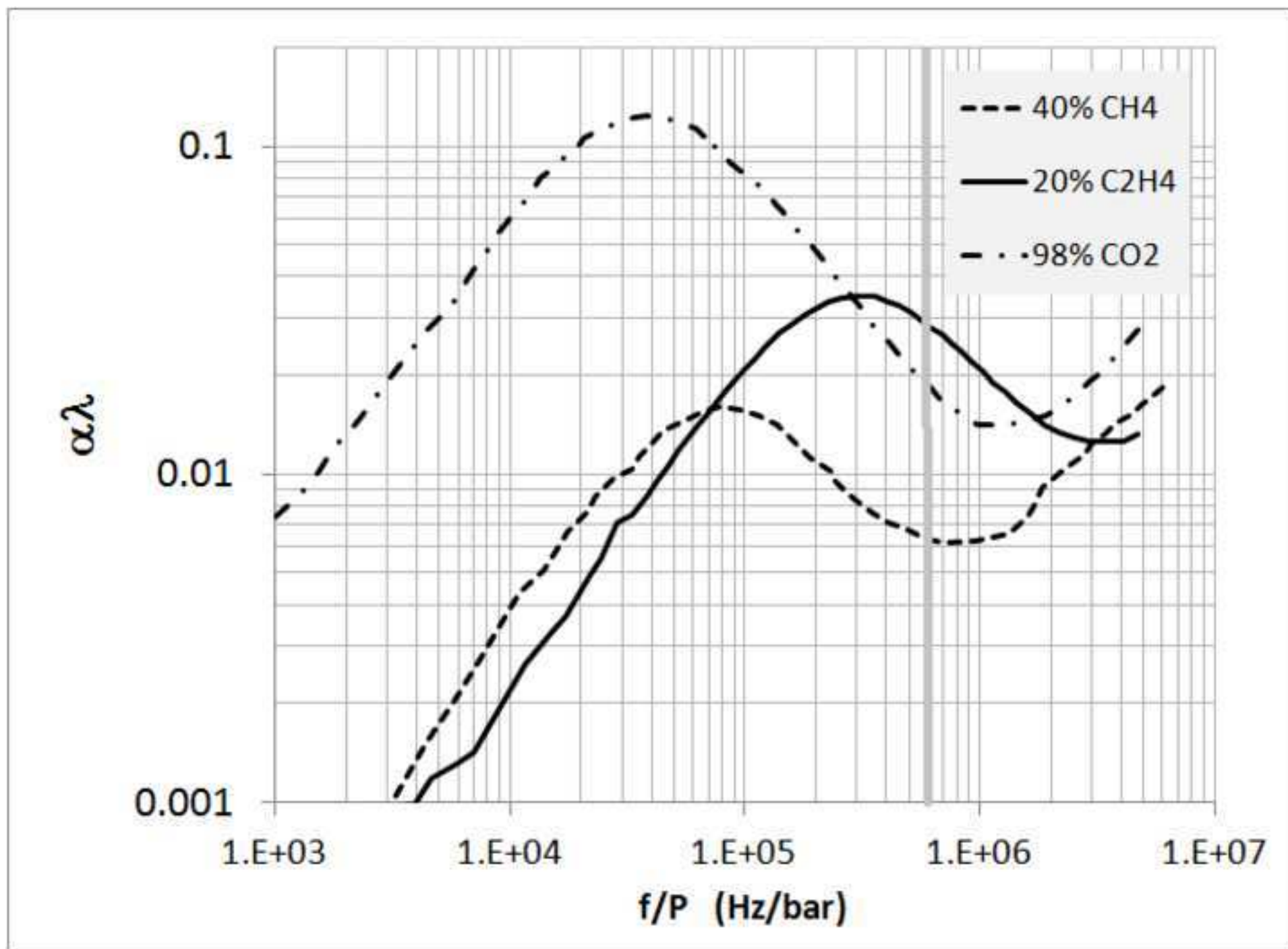


Figure
[Click here to download high resolution image](#)



Figure

[Click here to download high resolution image](#)

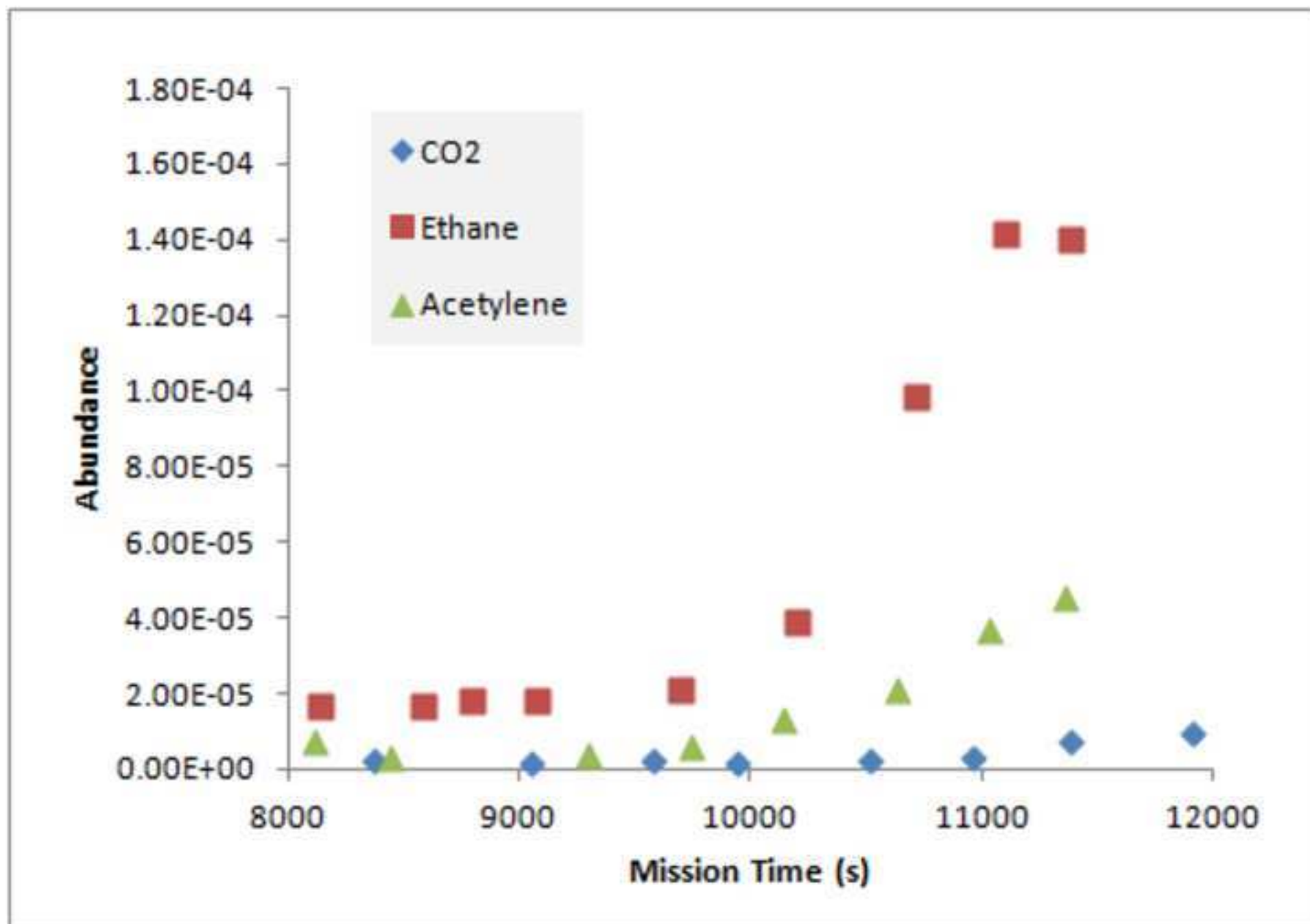


Figure
[Click here to download high resolution image](#)

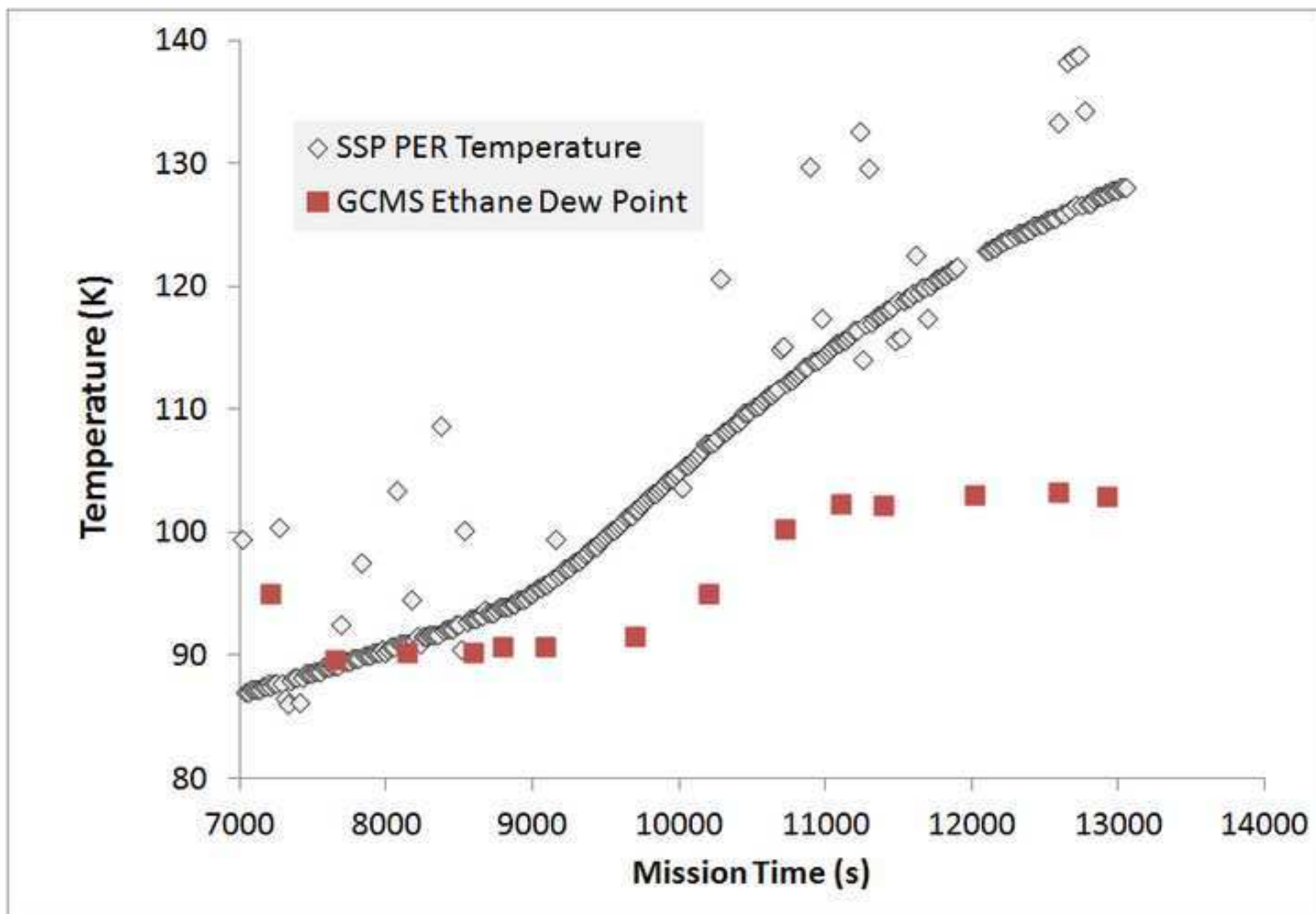


Figure
[Click here to download high resolution image](#)

